



## Abnormal asymmetry in benign epilepsy with unilateral and bilateral centrotemporal spikes: A combined fMRI and DTI study



Weifang Cao<sup>a,1</sup>, Yaodan Zhang<sup>b,1</sup>, Changyue Hou<sup>a</sup>, Fei Yang<sup>b</sup>, Jinnan Gong<sup>a</sup>, Sisi Jiang<sup>a</sup>, Yue Huang<sup>b</sup>, Ruhui Xiao<sup>b</sup>, Cheng Luo<sup>a,\*</sup>, Xiaoming Wang<sup>b,\*</sup>, Dezhong Yao<sup>a</sup>

<sup>a</sup> Key Laboratory for NeuroInformation of Ministry of Education, School of Life Science and Technology, University of Electronic Science and Technology of China, Chengdu, China

<sup>b</sup> Neurology Department, Affiliated Hospital of North Sichuan Medical College, North Sichuan Medical College, NanChong, China

### ARTICLE INFO

#### Keywords:

Benign epilepsy with centrotemporal spikes  
Functional magnetic resonance images  
Diffusion tensor imaging  
Asymmetry

### ABSTRACT

Benign epilepsy with centrotemporal spikes (BECTS) is the most common idiopathic focal childhood epilepsy associated with either unilateral or bilateral epileptic discharge. Asymmetry as an important characteristic of the human brain is beneficial for brain functions. However, little is known about on asymmetry of BECTS patients with different epileptic spikes pattern. In the present study, we investigated functional and structural asymmetries in unilateral spikes BECTS (U\_BECTS) patients and bilateral spikes BECTS (B\_BECTS) patients using resting state functional magnetic resonance images and diffusion tensor imaging. Compared with the controls, we observed a decreased voxel-mirrored interhemispheric functional connectivity (FC) in primary sensorimotor cortex (SM1) in U\_BECTS and B\_BECTS groups, and reduced fractional anisotropy (FA) values of the corpus callosum (CC) connecting bilateral SM1 were also observed in B\_BECTS group. Further region-based FC map analysis of SM1 demonstrated increased functional asymmetry with ipsilateral hemisphere, contralateral hemisphere and the whole brain in U\_BECTS and increased functional asymmetry with the contralateral hemisphere and the whole brain in B\_BECTS groups. The correlation between functional asymmetry of SM1 and intelligence quotient scores was found in the U\_BECTS group. The altered asymmetries of the SM1 further indicated the important role of SM1 in the pathophysiology of the BECTS. Furthermore, the B\_BECTS group also showed abnormal voxel-mirrored interhemispheric FC in the temporal pole, the lobule IX of the cerebellum, the caudate and the occipital cortex relative to the controls. Altogether, our findings provide additional insight into the neuronal mechanism of BECTS with different epileptic spikes pattern and cognitive impairments with BECTS patients.

### 1. Introduction

Benign epilepsy with centrotemporal spikes (BECTS) is a common idiopathic focal epilepsy syndromes in childhood and accounts for 13–25% of all cases of childhood epilepsy, with an onset between 3 and 13 years of age (Shields and Snead, 2009; Wirrell, 1998). The clinical manifestations include short-lasting facial sensory-motor symptoms, and neurophysiological studies indicate that the neural source of epileptic spikes is generally located in the primary sensorimotor cortices (Legarda et al., 1994; Panayiotopoulos et al., 2008). Among these discharges, approximately 60% are unilateral spikes, and 40% are bilateral spikes (Wirrell, 1998). Neuropsychological study has demonstrated that worse performances in nonverbal functions have also been reported in BECTS with bilateral or right spikes compared with those with left

spikes (Piccirilli et al., 1994). Neuroimaging studies have provided the evidence that epileptic discharges disturb the cerebral organization associating with functions, such as the bilateral representation of language network in BECTS patients with left spikes (Bedoin et al., 2011; Monjauze et al., 2011). These findings have shown the impact of the lateralization of epileptic focal activity on specific cerebral mechanisms, which may be important to cognitive impairments in BECTS patients (Bedoin et al., 2011; Bedoin et al., 2006), such as lower Wechsler Intelligence Scale and worse motor function (Garcia-Ramos et al., 2015; Overvliet et al., 2011).

Asymmetry is a characteristic of neuronal organization and is beneficial for functions in human (Toga and Thompson, 2003; Unterberger et al., 2016). Functional asymmetry, such as strong interhemispheric interaction of motor cortex in motor function and lateralized

\* Corresponding authors.

E-mail addresses: [chengluo@uestc.edu.cn](mailto:chengluo@uestc.edu.cn) (C. Luo), [wangxm238@163.com](mailto:wangxm238@163.com) (X. Wang).

<sup>1</sup> Weifang Cao and Yaodan Zhang are equaled to this work.

organization between the hemispheres in cognitive function, is crucial to healthy development across brain and is affected by disease processes (Stark et al., 2008). Magnetic resonance imaging (MRI), a non-invasive technique, provides us showing functional and structural asymmetry (Hugdahl, 2011). Recently, voxel-mirrored interhemispheric functional connectivity (FC), which examines the correlation of the time course between each pair of voxels in one hemisphere and its mirrored counterpart in the other using resting state functional MRI data, is used to investigate interhemispheric interaction and provides insights regarding disease processes and healthy development (Zuo et al., 2010). Aberrant interhemispheric FC asymmetry has been observed in generalized tonic-clonic seizures and mesial temporal lobe epilepsy (Ji et al., 2014; Yang et al., 2014). Conversely, FC map seeded at region of interest (ROI) reveals the relationship between the ROI and other brain regions, and is important to brain functions (Fox and Raichle, 2007). A neuroimaging study also investigates functional asymmetry of human brain by establishing that the two hemispheres have qualitatively different connections within- and between-hemispheres, and provides a direct evidence that asymmetry is associated with cognitive ability (Gotts et al., 2013). A FC map analysis seeded at an epileptic focus in frontal epilepsy shows altered functional network pattern and provide an understanding of seizure initiation and propagation (Luo et al., 2014). Thus, functional asymmetry provides a new approach to examine the effect of epileptic spikes on cerebral activity in BECTS patients. Furthermore, Diffusion tensor imaging (DTI) has been used to evaluate white matter tracts connecting brain regions affected by epileptic activity. Several DTI studies have reported the altered microstructure of the white matter in brain regions affected by the epileptic activity, especially in pre- and postcentral gyri and the corpus callosum (CC) (Ciumas et al., 2014; Kim et al., 2014; Xiao et al., 2014). Herein, we hypothesized that the functional and structural asymmetries were affected by the epileptic spikes of BECTS patients.

In the present study, all patients were divided into unilateral spikes BECTS (U\_BECTS) and bilateral spikes BECTS (B\_BECTS) patients. First, the functional asymmetry was investigated using the voxel-mirrored interhemispheric FC in the U\_BECTS, B\_BECTS and control groups. Then, the asymmetry based on the FC map was explored by seeding at regions that exhibited significant differences in the between-groups comparisons in the above analysis. Furthermore, the structural connectivity of the CC was examined using DTI analysis, because the CC, which is the largest commissural white matter pathway and an essential component for brain interhemispheric communication (Hugdahl, 2011), is also the major pathway for transferring seizure activities between two hemispheres (Unterberger et al., 2016). Finally, the relationship between asymmetry and clinical characteristics and cognitive performances was also analyzed in BECTS patients.

## 2. Methods

### 2.1. Participants

All BECTS patients were enrolled over a three-year period (from June 2012 to Aug 2015) from the pediatric epilepsy outpatient and inpatient department in Affiliated Hospital of North Sichuan Medical College, Nanchong, China. This study was reviewed and approved by the Ethical Committee of the Affiliated Hospital of North Sichuan Medical College, and all subjects (or their parents) provided informed consent for this study. All subjects underwent twenty-four-hour video-EEG recordings before diagnosis, and were sorted into unilateral spikes BECTS (U\_BECTS) and bilateral spikes BECTS (B\_BECTS). The inclusion criteria included (i) the diagnosis of BECTS patients were established in accordance with the criteria of the International League Against Epilepsy (ILAE) (Berg et al., 2010) by pediatric epileptologists (X.W., Y.Z., and Y.H.); (ii) no patients had other accompanying neurologic disorders, psychological disorders or brain lesions; (iii) normal brain MRI scans. The U\_BECTS subgroup consisted of 23 right-handed

patients, and the B\_BECTS subgroup consisted of 20 right-handed patients. Twenty-four right-handed, healthy subjects who were between 5 and 16 years of age were recruited as a control group. All of the subjects were individually evaluated using the Chinese version of the Wechsler Intelligence Scale for Children (WISC-III, <http://www.pearsonclinical.nl/tests>), including verbal conceptual reasoning (verbal intelligence quotient, VIQ), nonverbal reasoning (performance intelligence quotient, PIQ), and full scale intelligence quotient (FSIQ).

### 2.2. Image acquisition

All subjects were scanned using a 3T MRI scanner (MR750; GE Discovery,) with an eight-channel, standard, whole head coil. To minimize head motion, foam pads were used to fix the subjects' heads. Axial anatomical T1-weighted images acquisition used a 3-dimensional fast spoiled gradient echo (T1-3DFSPGR) sequence, generating 152 slices [echo time (TE) = 1.984 ms, repetition time (TR) = 6.008 ms, flap angle (FA) = 90°, matrix = 256 × 256, field of view (FOV) = 25.6 × 25.6 cm<sup>2</sup>, slice thickness (no gap) = 1 mm]. Resting state functional MRI data were acquired using gradient-echo EPI sequences (TR = 2000 ms, TE = 30 ms, FA = 90°, matrix = 64 × 64, FOV = 24 × 24 cm<sup>2</sup>, slice thickness = 4 mm (no gap), 32 slices per volume). All subjects underwent a 410 s resting state scan to yield 205 vols. To ensure magnetic field (B0) stabilization, the first five volumes were discarded. During the functional data scanning, the subjects were instructed to keep their eyes closed without falling asleep. The DTI acquisition used a single-shot spin-echo planar imaging sequence (matrix = 256 × 256, voxel size = 1.8 × 1.8 × 3 mm<sup>3</sup>, 50 slices covered the whole brain). One unweighted (b = 0 s/mm<sup>2</sup>) and 30 diffusion-weighted (b = 1000 s/mm<sup>2</sup>) image volumes were collected for 20 BECTS patients (10 B\_BECTS and 10 U\_BECTS) and 20 controls.

### 2.3. Functional images preprocessing

Functional imaging data were processed using the SPM8 software (<http://www.fil.ion.ucl.ac.uk/spm/>) and MATLAB Version 13a platforms (<http://www.mathworks.co.uk/products/matlab/>). First, functional images were corrected for the slice-timing and realigned for the head motion correction. The subjects with head motion that was greater than 2 mm of translation and 2° of rotation during scanning were excluded. In addition, the translation and rotation of the subjects were assessed by frame wise displacement (FD),  $FD_i = |\Delta d_{ix}| + |\Delta d_{iy}| + |\Delta d_{iz}| + |\Delta \alpha_i| + |\Delta \beta_i| + |\Delta \gamma_i|$ , where  $i$  is the  $i$ -th time point, and  $\Delta d_{ix} = d_{(i-1)x} - d_{ix}$  (similarly for the other head motion/rotation parameters).  $FD_0$  was set to zero and rotational displacements were converted from radians to millimeters. (Power et al., 2012) No significant differences were found among three groups in FD (mean ± SD, B\_BECTS 0.078 ± 0.041, U\_BECTS 0.07 ± 0.032, controls 0.097 ± 0.065,  $F = 1.57$ ,  $P = 0.217$ ). Next, the individual T1 images were coregistered to functional images and then segmented into gray matter (GM), cerebrospinal fluid (CSF), and white matter (WM). The resulting data were normalized to the MNI space, and these transformation parameters were applied to the functional images (resampled to 3 × 3 × 3 mm<sup>3</sup>). To account for differences in the geometric configuration between hemispheres, the preprocessed functional data were transformed to a symmetric space using a group-specific, symmetrical template, which was generated by all averaged and left-right mirrored normalized GM images. Finally, the functional images were spatially smoothed using an isotropic Gaussian kernel (6 mm full-width at half maximum).

### 2.4. Voxel-mirrored interhemispheric functional connectivity

Before FC analysis, linear trends and a phase-insensitive filter (0.01–0.08 Hz) were applied to reduce the effects of low frequency drift and high frequency physiological noise. Several nuisance signals,

including six head-motion parameters, WM signal, CSF signal, and global signal were regressed out using a general linear model. Then, Pearson's correlation coefficients were computed between the time courses of each pair of mirrored voxels in two hemispheres for each subject. The coefficients were assigned to the mirrored voxel. Then, voxel-mirrored interhemispheric FC map (Fisher's *r*-to-*z* transformed) was obtained for each subject. Finally, group-level analysis was produced using the random effect one-sample *t*-test in SPM8 for each group. Differences of voxel-mirrored interhemispheric FC among three groups (U\_BECTS, B\_BECTS and the controls) were analyzed using a one-way AVOVA ( $P < 0.01$ , cluster volume  $> 621 \text{ mm}^3$ ), and the post hoc two-sample *t*-test for each pair of groups ( $P < 0.005$ , cluster volume  $> 621 \text{ mm}^3$ ) with an explicit mask from the ANOVA analysis between groups.

## 2.5. Functional asymmetry of ROI-based FC map

To further explore FC asymmetry, we investigated asymmetry characteristics of FC maps of ROIs exhibiting significantly different voxel-mirrored interhemispheric FC. Because the ROIs were symmetric (i.e., the *m* ROIs are equivalent to *m*/2 pair of ROIs), the FC asymmetry were evaluated for each pair of ROIs. At first, Pearson's correlation coefficients were calculated between the mean time course of each ROI and the time course of all other voxels in the whole brain, and FC maps were obtained for each ROI and subject. To determine the connection pattern, FC maps were binarized according to the setting connection threshold. While considering that no other gold standard exists for setting the threshold of FC, we chose an ergodic correlation threshold that ranged from 0.3 to 0.75 at the intervals of 0.05. Voxels that were larger than the threshold were set to 1. Otherwise, they were set to 0. For a given ROI pair ( $X_r$  and  $X_l$ ), the number of voxels, which were larger than the threshold, was summed for the whole brain in the ipsilateral and contralateral hemispheres. Thus, there were six FC attributes for each ROI pair. For the right ROI ( $X_r$ ),  $N_{Rr}$  represents the number of suprathreshold connections in the right hemisphere with  $X_r$ ,  $N_{Lr}$  represents the number in the left hemisphere with  $X_r$ , and  $N_{Ar}$  represents the number in whole brain ( $N_{Rr} + N_{Lr}$ ). For the left ROI ( $X_l$ ),  $N_{Ll}$  represents the number of suprathreshold connections in the left hemisphere with  $X_l$ ,  $N_{Rl}$  represents the number in right hemisphere with  $X_l$ ,  $N_{Al}$  represents the number in the whole brain ( $N_{Rl} + N_{Ll}$ ).

Therefore, two asymmetry characteristics (sketched in Fig. 1), including asymmetry indexes (AIs) and lateralization indexes (LIs), were calculated based on these FC attributes:

1) The FC AIs of ROIs were defined using the following formula:

$$AI_{ipsi} = \frac{|C - A|}{C + A}$$

$$AI_{contra} = \frac{|D - B|}{D + B}$$

$$AI_{global} = \frac{|C + D - A - B|}{C + D + A + B}$$

$$LI_{ipsi} = \frac{C - A}{C + A}$$

$$LI_{contra} = \frac{D - B}{D + B}$$

$$LI_{global} = \frac{C + D - A - B}{C + D + A + B}$$

$$AI_{ipsi} = \frac{|N_{Rr} - N_{Ll}|}{N_{Rr} + N_{Ll}}; AI_{contra} = \frac{|N_{Lr} - N_{Rl}|}{N_{Rl} + N_{Lr}}; AI_{global} = \frac{|N_{Ar} - N_{Al}|}{N_{Al} + N_{Ar}};$$

$AI_{ipsi}$  ( $AI_{contra}$ ,  $AI_{global}$ ) is expressed as a continuous variable from 0 (i.e., the connection of right and left ROIs with ipsilateral hemispheric [contralateral hemispheric, all brain] voxels is equal) to 1 (i.e., either the right or left ROI has no connection with ipsilateral hemispheric [contralateral hemispheric, all brain] voxels). A larger value of  $AI_{ipsi}$  indicates a larger difference of FC between the right and left ROI with ipsilateral hemispheric voxels. Conversely, a lower value indicates a smaller difference.

2) The FC LIs of ROIs in B\_BECTS group and the controls were defined using the following formula:

$$LI_{ipsi} = \frac{N_{Rr} - N_{Ll}}{N_{Rr} + N_{Ll}}; LI_{contra} = \frac{N_{Lr} - N_{Rl}}{N_{Lr} + N_{Rl}}; LI_{global} = \frac{N_{Ar} - N_{Al}}{N_{Ar} + N_{Al}}$$

$LI_{ipsi}$  ( $LI_{contra}$ ,  $LI_{global}$ ) is expressed as a continuous variable from  $-1$  (i.e., the right ROI has no connection with ipsilateral hemispheric [contralateral hemispheric, all brain] voxels) to 1 (i.e., the left ROI has no connection with ipsilateral hemispheric [contralateral hemispheric, all brain] voxels). A value of  $LI_{ipsi}$  greater than zero represents the right lateralization of FC between the ROIs with ipsilateral hemispheric voxels, and a value less than 0 indicates left lateralization.

3) In U\_BECTS patients, we explored the FC lateralization of the ROI with the hemisphere ipsilateral ( $LI_{ipsi}$ ) and contralateral ( $LI_{contra}$ ) to spikes using the above formula. Here, we flipped the FC maps of U\_BECTS with left spikes; thus, all U\_BECTS were considered as the consistent epileptic focus with right spikes.

Before the statistical analysis of the ROI-based FC asymmetry, the normal distribution of values of asymmetry was tested for each group. Otherwise, variable transformation was used to normalize the values of the asymmetry. Differences among the three groups of AIs, one of ROI-based FC asymmetry characteristic, were analyzed using a one-way ANOVA following the post hoc two-sample *t*-test for each pair of groups. For the LIs of FC, thus, the other ROI-based FC asymmetry characteristic, we investigated the difference of between the B\_BECTS group and controls using a two-sample *t*-test. For the U\_BECTS group, one-sample *t*-test was used to compare the distribution of LI values against zero. All statistical threshold of P value was set at 0.05.

## 2.6. Diffusion tensor imaging analysis

Preprocessing of DTI data were carried out using the FMRIB Software Library (FSL; <http://www.fmrib.ox.ac.uk/fsl>). At first, the T1 eddy currents and head motion were corrected using affine registration

Fig. 1. Schematic of asymmetry characteristics of FC maps by seeding at  $X$ . There are two symmetry regions in both hemispheres:  $X_l$  and  $X_r$ . First, the functional connection maps with the regions  $X_l$  and  $X_r$  were calculated in whole brain respectively. The functional maps were divided into right and left hemispheres. Then, the number of voxels with suprathreshold connections was determined for each hemisphere like in this chart. Thus, A represents the number of suprathreshold connections in left hemisphere with  $X_l$ ; B represents the number in right hemisphere with  $X_l$ ; C represents the number of suprathreshold connections in right hemisphere with  $X_r$ ; D represents the number in left hemisphere with  $X_r$ . Final, six FC map attributes were defined.  $AI_{ipsi}$  represents FC asymmetry index of  $X$  with ipsilateral hemispheric voxels;  $AI_{contra}$  represents FC asymmetry index of  $X$  with contralateral hemispheric voxels;  $AI_{global}$  represents FC asymmetry index of  $X$  with all brain voxels;  $LI_{ipsi}$  represents FC lateralization index of  $X$  with ipsilateral hemispheric voxels;  $LI_{contra}$  represents FC lateralization index of  $X$  with contralateral hemispheric voxels;  $LI_{global}$  represents FC lateralization index of  $X$  with all brain voxels.

to the average image of three non-weighted images. Then, a diffusion tensor model was fitted to generate fractional anisotropy (FA) maps for each subject. To evaluate the effect of epileptic spikes on the structural connectivity of the CC in the BECTS patients, for each subject, 1) we drew the CC at individual's FA map manually. 2) The CC mask was used as the seed region for probabilistic tractography with five brain regions (i.e. frontal cortex, primary sensory-motor cortex (SM1), parietal cortex, occipital cortex and temporal cortex) in individual space as classification targets. 3) Hard segmentation of the CC region into five distinct subregions was performed according to the number of samples seeded from each voxel in CC reaching the five target mask respectively. 4) Deterministic tracking was performed for each CC subregion using Diffusion Toolkit (Mori et al., 1999) using an FA threshold of 0.2 and a maximum curvature of 300. Subjects whose streamline count was less than 20 were excluded in further analysis. Statistical analysis was performed using along-tract statistics (Colby et al., 2012). Before the statistical analysis, for each subject, the raw streamlines were re-parameterized using cubic B-spline curves. The streamlines are reoriented at the middle point of the two hemispheres and resampled with 100 vertices along their length in each hemisphere. The group differences of FA value at each point along the tract and at the entire track were carried out using ANOVAs ( $p < 0.05$ ) and the post hoc two-sample  $t$ -test for each pair of groups ( $p < 0.05$ ).

## 2.7. Clinical correlations

To explore the relationship between the neuroimaging measures and the clinical behavior features (age at onset, VIQ, PIQ, FSIQ) of BECTS, a partial correlation analysis was performed between all asymmetry and clinical behavior measurements controlling for age, gender and medicine.

## 3. Results

### 3.1. Demographic and neuropsychological test

Four BECTS and four control subjects were excluded due to excessive head motion, and one BECTS patient was excluded for a lack of raw data. Twenty U\_BECTS, 18 B\_BECTS and 20 controls were finally included for further functional asymmetry analysis. Only 20 BECTS patients and 20 controls underwent an MRI scans for DTI with the same scan protocols. The demographic, clinical and neuropsychological parameters for all 38 patients are shown in Table 1. Both the U\_BECTS and B\_BECTS groups showed significantly lower performance ( $p < 0.001$ ) on the WISC-III subscales relative to the controls (Table 1).

**Table 1**  
Demographic, clinical and neuropsychological test of all subjects.

	U_BECTS	B_BECTS	Controls	P value
Gender(male/female)	20(13/7)	18(9/9)	20(13/7)	0.558 <sup>a</sup>
Age(Year)	9.7 ± 2.02	9.14 ± 1.43	9.67 ± 2.55	0.663 <sup>b</sup>
Age at onset(Year)	8.72 ± 1.95	8.25 ± 1.86	–	0.461 <sup>c</sup>
WISC				
VIQ (Mean ± SD)	84.05 ± 5.95	81.67 ± 9.46	100.85 ± 5.86	< 0.001 <sup>b</sup>
PIQ (Mean ± SD)	94.8 ± 9.18	91.39 ± 12.54	115.62 ± 6.02	< 0.001 <sup>b</sup>
FSIQ (Mean ± SD)	87.65 ± 6.9	85 ± 10.89	108.46 ± 6.2	< 0.001 <sup>b</sup>

Abbreviations; U\_BECTS: benign focal epilepsy of childhood with centrottemporal spikes with unilateral spikes; B\_BECTS: benign focal epilepsy of childhood with centrottemporal spikes with bilateral spikes; WISC: Wechsler Intelligence Scale for Children; VIQ: Verbal Intelligence Quotient; PIQ: Performance Intelligence Quotient; FSIQ: Full Scale Intelligence Quotient.

<sup>a</sup> Chi-square test.

<sup>b</sup> one-way analysis of variance.

<sup>c</sup> two-sample  $t$ -test.

### 3.2. Voxel-mirrored interhemispheric functional connectivity

ANOVA analysis showed between-groups differences of voxel-mirrored interhemispheric FC in the primary sensorimotor cortex (SM1), the temporal pole (TP), the lobule IX of the cerebellum, the caudate and the occipital cortex (Fig. 2, Table 2). The post-hoc  $t$ -tests indicated that U\_BECTS group exhibited decreased voxel-mirrored interhemispheric FC in SM1 compared with the controls, while B\_BECTS group exhibited a decreased voxel-mirrored interhemispheric FC in SM1 and the occipital cortex and increased voxel-mirrored interhemispheric FC in the TP and the lobule IX of the cerebellum and the caudate relative to the controls (Fig. 2). However, no significant differences of voxel-mirrored interhemispheric FC were found between the B\_BECTS and U\_BECTS groups.

### 3.3. FC asymmetry of ROI-based FC map

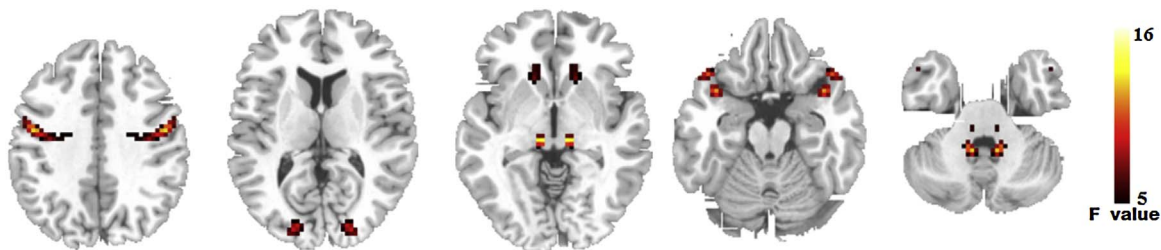
According to the significant differences of voxel-mirrored interhemispheric FC between groups, five pairs of ROIs (bilateral SM1, the TP, the caudate, the occipital cortex and the lobule IX of the cerebellum) were chosen for the further ROI-based FC asymmetry analysis. Because the high threshold might result in a null connection to the contralateral hemisphere (such as  $N_{Lr}$  or  $N_{Rl} = 0$ ,  $N_{Rr}/N_{Rl}$  represents the number of suprathreshold connections in the right/left hemisphere with left/right ROI), the minimum cluster size of connections was defined for this case. In addition, 10 voxels was set to avoid strange voxels. According to this rule, the connection threshold to the ipsilateral hemisphere and the whole brain ranged from 0.3 to 0.75 at the intervals of 0.05, but the connection threshold to contralateral hemisphere ranged from 0.3 to 0.6 at the intervals of 0.05.

For AIs, an ANOVA analysis showed significant differences in SM1. Further post-hoc analyses showed increases in all AIs of SM1 in U\_BECTS, and increased  $AI_{contra}$  and  $AI_{global}$  of SM1 in B\_BECTS compared to the controls (Fig. 3). The two BECTS groups show no significant differences in all AIs. For LIs, B\_BECTS group showed decreased  $LI_{ipsi}$  and  $LI_{global}$  of the TP relative to the controls (Fig. 3). In U\_BECTS group, the FC lateralization did not reach statistical significance.

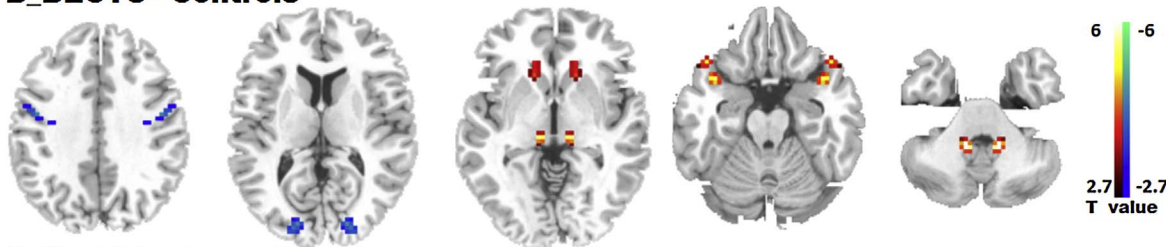
### 3.4. Diffusion tensor imaging

Eleven controls, 5 U\_BECTS and 5 B\_BECTS patients were included in the statistical analysis while streamline counts were more than 20. An ANOVA analysis showed that the CC connecting to the bilateral SM1 had significant group interactions while more than 10 successive points along the tract were set (Fig. 4). Post-hoc test analysis indicated that the B\_BECTS group exhibited lower FA relative to U\_BECTS group (Fig. 4). For the tract connecting to bilateral SM1, no group differences were found when FA values were averaged across the entire tract.

**(a) Differences among 3 groups**



**(b) B\_BECTS - Controls**



**(c) U\_BECTS - Controls**

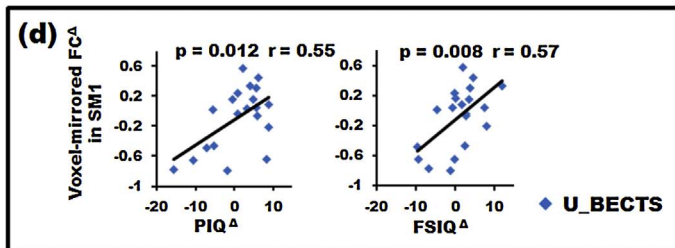
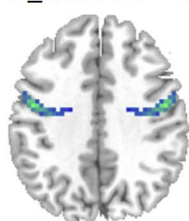


**Fig. 2.** Results of the voxel-mirrored interhemispheric functional connectivity between groups by one-way ANOVA analysis ( $p < 0.01$ , cluster size  $> 621 \text{ mm}^3$ ) (a), and a post-hoc test between two BECTS groups and the controls ( $P < 0.005$ , cluster size  $> 621 \text{ mm}^3$ ) (b, c); the negative correlation between voxel-mirrored interhemispheric FC in SM1 and PIQ and FSIQ in U\_BECTS group (d).  $\Delta$ in scatter diagram represents the adjusted values controlling for the influence of the gender, age and AEDs (linear regression with covariates including gender, age and AEDs). PIQ: Performance Intelligence Quotient; FSIQ: Full Scale Intelligence Quotient.

**Table 2**  
Significant difference of voxel-mirrored interhemispheric functional connectivity among two BECTS groups and the controls by an ANOVA analysis ( $p < 0.01$ , cluster size  $> 621 \text{ mm}^3$ ).

Brain Regions	Brodmann Area (BA)	MNI coordinate <sup>a</sup>			F value	Cluster size (mm <sup>3</sup> )
		X	Y	Z		
Lobule IX of the cerebellum		12	-51	-39	16.83	1269
Primary sensorimotor cortex	BA 6	48	-9	33	13.10	4374
Temporal Pole	BA 38	39	9	-27	13.05	1701
Occipital cortex	BA18	21	-93	9	8.78	648
Caudate		15	18	-9	7.35	783

<sup>a</sup> The coordinate of regions in the right hemisphere (the regions of significant difference are symmetric, and the coordinate of regions in the left hemisphere was not listed in the table).

**3.5. Clinical correlations**

The significant positive correlation between voxel-mirrored interhemispheric FC of SM1 and PIQ and FSIQ were observed in U\_BECTS patients, controlling for age, gender and medicine (Fig. 2d). Regarding the ROI-based FC asymmetry, we averaged the AIs and LIs over the range of connection thresholds (the connection threshold to the ipsilateral hemisphere and the whole brain ranged from 0.3 to 0.75; the connection threshold to the contralateral hemisphere ranged from 0.3 to 0.6). The relationship between the average AIs and LIs and the clinical and neuropsychological measures were examined using partial

correlation analysis. In U\_BECTS, a negative correlation was found between the  $AI_{ipsi}$  and  $AI_{global}$  of the SM1 and PIQ and FSIQ (Fig. 5). In the B\_BECTS group, a negative correlation was found between the  $LI_{ipsi}$  and  $LI_{global}$  of the TP and PIQ (Fig. 5). However, no significant correlation between neuroimaging measures and age at onset was observed in BECTS patients.

**4. Discussion**

The present study explored the functional and structural asymmetries in both U\_BECTS and B\_BECTS groups using resting-state fMRI and DTI. We made two observations. First, compared to the controls, both U\_BECTS and B\_BECTS groups demonstrated an altered voxel-mirrored interhemispheric FC in SM1, and the lower FA value of the CC connecting bilateral SM1 was also found in B\_BECTS group relative to the U\_BECTS group; further ROI-based FC map analysis showed increased  $AI_{ipsi}$ ,  $AI_{contra}$  and  $AI_{global}$  of SM1 in the U\_BECTS group and increased  $AI_{contra}$  and  $AI_{global}$  of SM1 in the B\_BECTS group. The correlation between functional asymmetry in SM1 and IQ was found in the U\_BECTS group. Second, B\_BECTS group also demonstrated abnormal voxel-mirrored interhemispheric FC in the TP, the caudate and the lobule IX of the cerebellum and the occipital cortex, and the FC map analysis showed a decreased  $LI_{ipsi}$  and  $LI_{global}$  in the TP. Furthermore, a negative correlation between the  $LI_{ipsi}$  and  $LI_{global}$  in the TP and PIQ was found in the B\_BECTS group. These findings, altered asymmetry in BECTS patients particularly in the SM1, provided a better understanding of the pathophysiology of the BECTS with different epileptic pattern.

Previous research has demonstrated that the epileptogenic zone is located in the primary sensorimotor cortices (Boor et al., 2007; Legarda

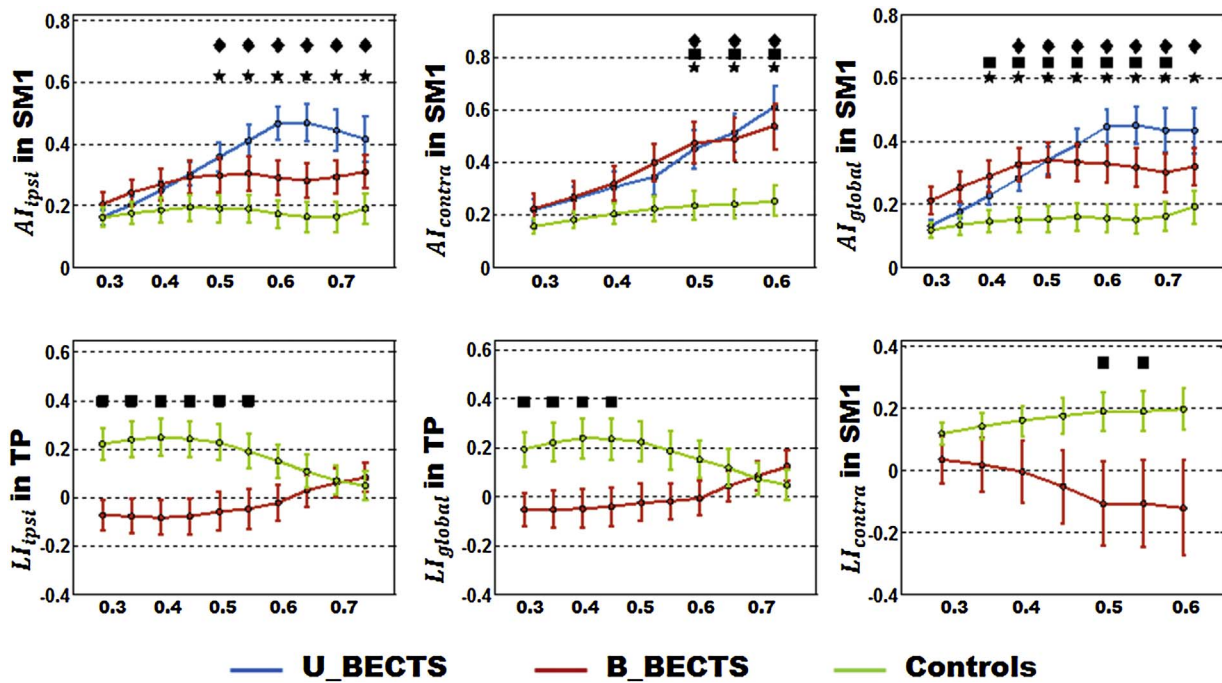


Fig. 3. Significant differences of AIs (upper row) and Lis (lower row). Pentagram represents significant difference between groups by one-way ANOVA, diamond represents significant difference between the U\_BECS group and the controls by two-sample *t*-test; square represents significant difference between the B\_BECS group and the controls by two-sample *t*-test. AI: asymmetry index; B\_BECS: bilateral spikes BECS; SM1: primary sensorimotor cortex; LI: lateralization index; TP: temporal pole; U\_BECS: unilateral spikes BECS.

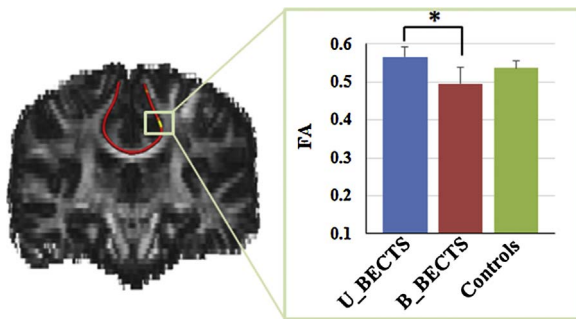


Fig. 4. Tracts with significant group differences in the corpus callosum (CC) connecting bilateral primary sensorimotor cortex (SM1) are shown. The locations of significant differences among 3 groups (one-way ANOVA analysis,  $p < 0.05$  and 13 successive points along the tract) are indicated with light green rectangle and significant differences of the mean fractional anisotropy (FA) values among 3 groups are shown in the left histogram (\*  $p < 0.05$ ). B\_BECS: bilateral spikes BECS; U\_BECS: unilateral spikes BECS. (For interpretation of the references to colour in this figure legend, the reader is referred to the web version of this article.)

et al., 1994). Here, both the U\_BECS and B\_BECS patients showed decreased voxel-mirrored interhemispheric FC in the SM1, which was concordant with the epileptogenic zone that included localization, as indicated by the EEG and EEG-fMRI measures. Recent neuroimaging studies have reported functional abnormalities with regard to local activity (Tang et al., 2014; Wu et al., 2015; Zhu et al., 2015) and functional integration of networks (Ji et al., 2016; Koelewijn et al., 2015; Luo et al., 2015; Xiao et al., 2015), which support the functional abnormalities of the sensorimotor cortex in BECS patients. In the present study, both BECS groups demonstrated decreased voxel-mirrored interhemispheric FC in SM1, although the BECS patients with bilateral spikes were distinguished from those with unilateral spikes. Evidences from fMRI studies revealed the strongest interhemispheric FC in sensorimotor cortex during brain development (Zuo et al., 2010). Thus, decreased voxel-mirrored interhemispheric FC in SM1 found in two BECS groups suggested that interhemispheric connectivity between bilateral SM1 was prone to be affected by either unilateral or

bilateral epileptic activity. Furthermore, we observed a positive correlation between voxel-based interhemispheric FC of SM1 and PIQ and FSIQ in U\_BECS patients.

The CC, which provided a pathway for communication between the two hemisphere, was believed to be involved in the propagation of epileptic activities (Unterberger et al., 2016). In the present study, we also evaluated the structural asymmetry of the CC connecting to interhemispheric regions in the BECS patients using along-tract statistics, and found reduced FA values of the CC connecting to bilateral SM1 in the B\_BECS group relative to U\_BECS group. Recent several DTI studies have found altered microstructure of WM including the CC and epileptic foci (i.e. SM1) in BECS patients (Ciumas et al., 2014; Kim et al., 2014; Xiao et al., 2014). Our finding added to the evidence that the white matter microstructure of the CC was affected by epileptic activity. Here, lower FA values of the CC connecting to bilateral SM1 in the B\_BECS group relative to U\_BECS group might suggest that the bilateral repetitive seizures affect white matter microstructure more seriously. Altogether, our findings, altered voxel-mirrored interhemispheric FC and fiber connectivity in SM1, might be associated with BECS.

To further investigate the FC asymmetry, we computed asymmetry characteristics of FC maps of regions exhibiting different voxel-based FC with voxels in the ipsilateral hemisphere, the contralateral hemisphere and the whole brain. We observed significantly altered FC asymmetry of SM1 between groups. Increased  $AI_{contra}$  and  $AI_{global}$  of SM1 (here, increased  $AI_{contra}$  represents that FC strength of bilateral SM1 with voxels of contralateral hemisphere is different, i.e., FC pattern of bilateral SM1 is more asymmetric) were observed in the U\_BECS and B\_BECS groups, but increased the  $AI_{ipsi}$  in SM1 was only observed in the U\_BECS group. Moreover, the FC lateralization was also examined to reveal the impact of epileptic spikes lateralization on the side-oriented FC lateralization, and the decreased  $LI_{contra}$  in SM1 was found in B\_BECS group relative to the controls. For the U\_BECS group, the lateralization of FC maps in the hemisphere ipsilateral and contralateral to spikes was explored and did not reach statistical significance. FC asymmetry, qualitative patterns of lateralized cortical interactions within- and between-hemispheres, can be beneficial for

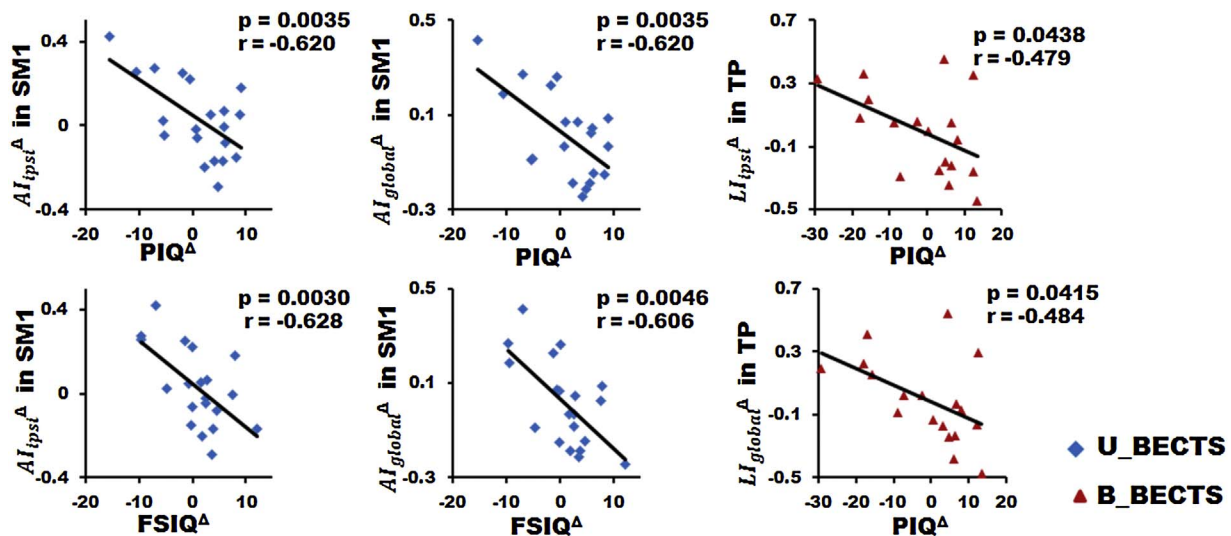


Fig. 5. Results of correlation between FC asymmetry characteristics and cognitive performances.  $\Delta$  represents the adjusted values controlling for the influence of the gender, age and AEDs (linear regression with covariates including gender, age and AEDs). AI: asymmetry index; B\_BECTS: bilateral spikes BECTS; SM1: primary sensorimotor cortex; FSIQ: Full Scale Intelligence Quotient; LI: lateralization index; PIQ: Performance Intelligence Quotient; TP: temporal pole; U\_BECTS: unilateral spikes BECTS.

brain function, such as cognitive ability (Gotts et al., 2013). Neuroimaging studies have reported that the SM1 was also involved in cognitive function, except for motor function (Fox et al., 2006). Negative correlation between the  $AI_{ipsi}$  and  $AI_{global}$  of SM1 and PIQ and FSIQ was observed in the U\_BECTS group. Here, we observed the correlation only in the U\_BECTS group. We speculated that the unilateral epileptic discharge mainly affected the ipsilateral hemispheric regions. Therefore, the U\_BECTS patients might show more significant alteration of the functional asymmetries than the B\_BECTS patients. In addition, the correlation analysis was evaluated by the average of the AIs and LIs over the range of connection thresholds, and the use of an average might affect the correlation analysis. Taken together, these findings, the altered functional asymmetry of SM1 in two BECTS subgroups as expected, might improve understanding of the neuronal mechanisms of the BECTS patients with different epileptic spikes pattern and were associated with impaired cognitive function in BECTS patients.

Although BECTS is a positive prognosis for seizure remission, researchers have documented impaired cognitive function in BECTS patients (Cerminara et al., 2010; Garcia-Ramos et al., 2015). We observed abnormal voxel-mirrored interhemispheric FC of cognitive-related regions (i.e. the TP, the caudate and the lobule IX of the cerebellum) and the decreased  $LI_{ipsi}$  and  $LI_{global}$  of the TP in the B\_BECTS group compared to the controls. Here, a decreased  $LI_{ipsi}$  of the TP represented that FC of bilateral TP with voxels in ipsilateral hemisphere had less asymmetrical pattern. The TP has been known to be involved in language function and social cognition system and was influenced by neurological diseases (Blaizot et al., 2010; Olson et al., 2007). The alteration of local activity in the TP was also found in other studies of BECTS (Tang et al., 2014). Furthermore, negative correlation between  $LI_{ipsi}$  and  $LI_{global}$  of the TP and PIQ was also found in the B\_BECTS group. Studies of the corticostriatal circuitry have been verified the caudate associating with cognitive function except for motor function (Grahm et al., 2008). Neuroimaging studies also demonstrated that BECTS affected striatal function and structure in striatum (Lin et al., 2012; Luo et al., 2015). The lobule IX of the cerebellum, which was believed to connect with the DMN (Habas et al., 2009), was also found to be abnormal in B\_BECTS group. Taken together, these wide altered asymmetries suggested the effects of bilateral epileptic spikes on asymmetry in B\_BECTS patients, and were associated with cognitive impairment in BECTS patients.

Several limitations should be noted in the present study. First, our findings highlighted the functional and structural interhemispheric asymmetry of the BECTS patients with unilateral and bilateral spikes,

but diagnosed focus may not be considered absolute and definitive due to its propagation. Second, the asymmetric cortical structure was transformed to the spatial symmetric template to gain the spatial corresponding regions. Third, the use of antiepileptic drugs can affect the brain activity of patients. Therefore, further studies concerning homogenous patients are needed. Fourth, the relative small sample size would be a shortage of the DTI study. In the future, more subjects are necessary to verify the altered structural connectivity of the CC. Fourth, additional neuropsychological tests (e.g. the motor performances) are needed to investigate the correlation between cognitive dysfunction and asymmetry deficits.

## 5. Conclusion

The altered functional and structural asymmetry of the SM1 found in both BECTS group further indicated the key role of the SM1 in the pathophysiology of the BECTS. Furthermore, the B\_BECTS group exhibited abnormal asymmetry in wide brain regions (including the TP, caudate, lobule IX of the cerebellum). In addition, we also found a correlation between functional asymmetry of SM1 and FIQ and FSIQ in the U\_BECTS group and between FC asymmetry of the TP and FIQ and FSIQ in the B\_BECTS group. Our findings might provide additional insight into the neuronal mechanisms of BECTS with different epileptic spikes pattern and cognitive impairments with BECTS patients.

## Declaration of interest

None.

## Acknowledgments

We are grateful to all the participants in this study: W.C., C.L. X.W. and D.Y. conceived and designed this study. X.W., Y.Z., F.Y. and R.X. diagnosed the subjects. C.H., W.C., J.G., S.J. and Y.H. analyzed the data. W.C., C.L., W.C., C.H. and J.G. prepared the figures and tables. X.W., and D.Y. wrote the main manuscript text. All authors reviewed the manuscript.

This work was supported by grants from the National Nature Science Foundation of China [81271547, 91232725, 81371636, 81471638], the PCSIRT project [IRT0910], and The “111” project [No. B12027].

## References

- Bedoin, N., Herbillon, V., Lamoury, I., Arthaud-Garde, P., Ostrowsky, K., De Bellescize, J., Keo Kosal, P., Damon, G., Rousselle, C., 2006. Hemispheric lateralization of cognitive functions in children with centrotemporal spikes. *Epilepsy Behav.* 9, 268–274.
- Bedoin, N., Ferragne, E., Lopez, C., Herbillon, V., De Bellescize, J., des Portes, V., 2011. Atypical hemispheric asymmetries for the processing of phonological features in children with rolandic epilepsy. *Epilepsy Behav.* 21, 42–51.
- Berg, A.T., Berkovic, S.F., Brodie, M.J., Buchhalter, J., Cross, J.H., van Emde Boas, W., Engel, J., French, J., Glauser, T.A., Mathern, G.W., Moshe, S.L., Nordli, D., Plouin, P., Scheffer, I.E., 2010. Revised terminology and concepts for organization of seizures and epilepsies: report of the ILAE Commission on Classification and Terminology, 2005–2009. *Epilepsia* 51, 676–685.
- Blaizot, X., Mansilla, F., Insausti, A.M., Constans, J.M., Salinas-Alaman, A., Pro-Sistiaga, P., Mohedano-Moriano, A., Insausti, R., 2010. The human parahippocampal region: i: Temporal pole cytoarchitectonic and MRI correlation. *Cereb. Cortex* 20, 2198–2212.
- Boor, R., Jacobs, J., Hinzmann, A., Bauermann, T., Scherg, M., Boor, S., Vucurevic, G., Pfeleiderer, C., Kutschke, G., Stoeter, P., 2007. Combined spike-related functional MRI and multiple source analysis in the non-invasive spike localization of benign rolandic epilepsy. *Clin. Neurophysiol.* 118, 901–909.
- Cerminara, C., D'Agati, E., Lange, K.W., Kaunzinger, L., Tucha, O., Parisi, P., Spalice, A., Curatolo, P., 2010. Benign childhood epilepsy with centrotemporal spikes and the multicomponent model of attention: a matched control study. *Epilepsy Behav.* 19, 69–77.
- Ciomas, C., Saignavongs, M., Ilski, F., Herbillon, V., Laurent, A., Lothe, A., Heckemann, R.A., de Bellescize, J., Panagiotakaki, E., Hannoun, S., Marinier, D.S., Montavont, A., Ostrowsky-Coste, K., Bedoin, N., Rylvlin, P., 2014. White matter development in children with benign childhood epilepsy with centro-temporal spikes. *Brain*.
- Colby, J.B., Soderberg, L., Lebel, C., Dinov, I.D., Thompson, P.M., Sowell, E.R., 2012. Along-tract statistics allow for enhanced tractography analysis. *Neuroimage* 59, 3227–3242.
- Fox, M.D., Raichle, M.E., 2007. Spontaneous fluctuations in brain activity observed with functional magnetic resonance imaging. *Nat. Rev. Neurosci.* 8, 700–711.
- Fox, M.D., Corbetta, M., Snyder, A.Z., Vincent, J.L., Raichle, M.E., 2006. Spontaneous neuronal activity distinguishes human dorsal and ventral attention systems. *Proc. Natl. Acad. Sci. U. S. A.* 103, 10046–10051.
- Garcia-Ramos, C., Jackson, D.C., Lin, J.J., Dabbs, K., Jones, J.E., Hsu, D.A., Stafstrom, C.E., Zawadzki, L., Seidenberg, M., Prabhakaran, V., Hermann, B.P., 2015. Cognition and brain development in children with benign epilepsy with centrotemporal spikes. *Epilepsia*.
- Gotts, S.J., Jo, H.J., Wallace, G.L., Saad, Z.S., Cox, R.W., Martin, A., 2013. Two distinct forms of functional lateralization in the human brain. *Proc. Natl. Acad. Sci. U. S. A.* 110, E3435–3444.
- Grahn, J.A., Parkinson, J.A., Owen, A.M., 2008. The cognitive functions of the caudate nucleus. *Prog. Neurobiol.* 86, 141–155.
- Habas, C., Kamdar, N., Nguyen, D., Prater, K., Beckmann, C.F., Menon, V., Greicius, M.D., 2009. Distinct cerebellar contributions to intrinsic connectivity networks. *J. Neurosci.* 29, 8586–8594.
- Hugdahl, K., 2011. Hemispheric asymmetry: contributions from brain imaging. *Wiley Interdiscip. Rev. Cognit. Sci.* 2, 461–478.
- Ji, G.J., Zhang, Z., Xu, Q., Zang, Y.F., Liao, W., Lu, G., 2014. Generalized tonic-clonic seizures: aberrant interhemispheric functional and anatomical connectivity. *Radiology* 271, 839–847.
- Ji, G.-J., Yu, Y., Miao, H.-H., Wang, Z.-J., Tang, Y.-L., Liao, W., 2016. Decreased network efficiency in benign epilepsy with centrotemporal spikes. *Radiology* 160422.
- Kim, S.E., Lee, J.H., Chung, H.K., Lim, S.M., Lee, H.W., 2014. Alterations in white matter microstructures and cognitive dysfunctions in benign childhood epilepsy with centrotemporal spikes. *Eur. J. Neurol.* 21, 708–717.
- Koelwijn, L., Hamandi, K., Brindley, L.M., Brookes, M.J., Routley, B.C., Muthukumaraswamy, S.D., Williams, N., Thomas, M.A., Kirby, A., Te Water Naude, J., Gibbon, F., Singh, K.D., 2015. Resting-state oscillatory dynamics in sensorimotor cortex in benign epilepsy with centro-temporal spikes and typical brain development. *Hum. Brain Mapp.*
- Legarda, S., Jayakar, P., Duchowny, M., Alvarez, L., Resnick, T., 1994. Benign rolandic epilepsy: high central and low central subgroups. *Epilepsia* 35, 1125–1129.
- Lin, J.J., Riley, J.D., Hsu, D.A., Stafstrom, C.E., Dabbs, K., Becker, T., Seidenberg, M., Hermann, B.P., 2012. Striatal hypertrophy and its cognitive effects in new-onset benign epilepsy with centrotemporal spikes. *Epilepsia* 53, 677–685.
- Luo, C., An, D., Yao, D., Gotman, J., 2014. Patient-specific connectivity pattern of epileptic network in frontal lobe epilepsy. *Neuroimage Clin.* 4, 668–675.
- Luo, C., Zhang, Y., Cao, W., Huang, Y., Yang, F., Wang, J., Tu, S., Wang, X., Yao, D., 2015. Altered structural and functional feature of striato-Cortical circuit in benign epilepsy with centrotemporal spikes. *Int. J. Neural Syst.* 25, 1550027.
- Monjauze, C., Broadbent, H., Boyd, S.G., Neville, B.G., Baldeweg, T., 2011. Language deficits and altered hemispheric lateralization in young people in remission from BECTS. *Epilepsia* 52, e79–83.
- Mori, S., Crain, B.J., Chacko, V.P., van Zijl, P.C., 1999. Three-dimensional tracking of axonal projections in the brain by magnetic resonance imaging. *Ann. Neurol.* 45, 265–269.
- Olson, I.R., Plotzker, A., Ezzyat, Y., 2007. The Enigmatic temporal pole: a review of findings on social and emotional processing. *Brain* 130, 1718–1731.
- Overvliet, G.M., Aldenkamp, A.P., Klinkenberg, S., Nicolai, J., Vles, J.S., Besseling, R.M., Backes, W., Jansen, J.F., Hofman, P.A., Hendriksen, J., 2011. Correlation between language impairment and problems in motor development in children with rolandic epilepsy. *Epilepsy Behav.* 22, 527–531.
- Panayiotopoulos, C.P., Michael, M., Sanders, S., Valeta, T., Koutroumanidis, M., 2008. Benign childhood focal epilepsies: assessment of established and newly recognized syndromes. *Brain* 131, 2264–2286.
- Piccirilli, M., D'Alessandro, P., Sciarma, T., Cantoni, C., Dioguardi, M.S., Giuglietti, M., Iba, A., Tiacci, C., 1994. Attention problems in epilepsy: possible significance of the epileptogenic focus. *Epilepsia* 35, 1091–1096.
- Power, J.D., Barnes, K.A., Snyder, A.Z., Schlaggar, B.L., Petersen, S.E., 2012. Spurious but systematic correlations in functional connectivity MRI networks arise from subject motion. *Neuroimage* 59, 2142–2154.
- Shields, W.D., Snead 3rd, O.C., 2009. Benign epilepsy with centrotemporal spikes. *Epilepsia* 50 (Suppl 8), 10–15.
- Stark, D.E., Margulies, D.S., Shehzad, Z.E., Reiss, P., Kelly, A.M., Uddin, L.Q., Gee, D.G., Roy, A.K., Banich, M.T., Castellanos, F.X., Milham, M.P., 2008. Regional variation in interhemispheric coordination of intrinsic hemodynamic fluctuations. *J. Neurosci.* 28, 13754–13764.
- Tang, Y.L., Ji, G.J., Yu, Y., Wang, J., Wang, Z.J., Zang, Y.F., Liao, W., Ding, M.P., 2014. Altered regional homogeneity in rolandic epilepsy: a resting-state fMRI study. *BioMed Res. Int.* 2014, 960395.
- Toga, A.W., Thompson, P.M., 2003. Mapping brain asymmetry. *Nat. Rev. Neurosci.* 4, 37–48.
- Unterberger, I., Bauer, R., Walsler, G., Bauer, G., 2016. Corpus callosum and epilepsies. *Seizure* 37, 55–60.
- Wirrell, E.C., 1998. Benign epilepsy of childhood with centrotemporal spikes. *Epilepsia* 39 (Suppl 4), S32–41.
- Wu, Y., Ji, G.J., Zang, Y.F., Liao, W., Jin, Z., Liu, Y.L., Li, K., Zeng, Y.W., Fang, F., 2015. Local activity and causal connectivity in children with benign epilepsy with centrotemporal spikes. *PLoS One* 10, e0134361.
- Xiao, F., Chen, Q., Yu, X., Tang, Y., Luo, C., Fang, J., Liu, L., Huang, X., Gong, Q., Zhou, D., 2014. Hemispheric lateralization of microstructural white matter abnormalities in children with active benign childhood epilepsy with centrotemporal spikes (BECTS): A preliminary DTI study. *J. Neurol. Sci.* 336, 171–179.
- Xiao, F., Lei, D., An, D., Li, L., Chen, S., Chen, F., Yang, T., Ren, J., Huang, X., Gong, Q., Zhou, D., 2015. Functional brain connectome and sensorimotor networks in rolandic epilepsy. *Epilepsy Res.* 113, 113–125.
- Yang, T., Ren, J., Li, Q., Li, L., Lei, D., Gong, Q., Zhou, D., 2014. Increased interhemispheric resting-state in idiopathic generalized epilepsy with generalized tonic-clonic seizures: a resting-state fMRI study. *Epilepsy Res.* 108, 1299–1305.
- Zhu, Y., Yu, Y., Shinkareva, S.V., Ji, G.J., Wang, J., Wang, Z.J., Zang, Y.F., Liao, W., Tang, Y.L., 2015. Intrinsic Brain Activity as a Diagnostic Biomarker in Children with Benign Epilepsy with Centrotemporal Spikes. *Hum. Brain Mapp.* 36, 3878–3889.
- Zuo, X.N., Kelly, C., Di Martino, A., Mennes, M., Margulies, D.S., Bangaru, S., Grzadzinski, R., Evans, A.C., Zang, Y.F., Castellanos, F.X., Milham, M.P., 2010. Growing together and growing apart: regional and sex differences in the lifespan developmental trajectories of functional homotopy. *J. Neurosci.* 30, 15034–15043.